INTERNATIONAL JOURNAL of RENEWABLE ENERGY RESEARCH
Hoa M. Nguyen and Hoan V. Pham, Vol.10, No.4, December, 2020

Local Volt/VAR Droop Control Strategies for Wind Generators in Distribution Networks

Hoa M. Nguyen*, Hoan V. Pham*‡

*Department of Electrical Engineering, Tra Vinh University, Vietnam

(hoatvu@tvu.edu.vn, pham.v.hoan@tvu.edu.vn)

‡ Corresponding Author: Hoan V. Pham, Department of Electrical Engineering, Tra Vinh University, Vietnam, Tel: +84 294 3855246,

Fax: +84 294 3855217, pham.v.hoan@tvu.edu.vn

Received: 02.11.2020 Accepted: 06.12.2020

Abstract- This paper proposes a novel approach using a non-linear least squares method for fitting optimally statistical data points to estimate optimal set-points of various local Volt/var droop control schemes implemented into wind generators (WGs) in distribution networks. The approach utilizes the Monte Carlo simulation and considers the variation of wind speed, electricity demand, and outage duration of WGs as uncertainties to evaluate the effects of each local scheme regarding the resulting statistical attributes of voltage variation profiles and total active power losses. The approach's effectiveness is demonstrated on a radial distribution network in Germany with four identical 20 kV feeders.

Keywords Distribution networks, loss reduction, Mean-variance mapping optimization.

1. Introduction

Nowadays towards the smart grids, most voltage control methods require a high level of communication between the components of the system, thus incurring high costs in its implementation. Since each method has its benefits and drawbacks and an engineering solution based on the equilibrium between cost and technical impact is needed, local control methods such as constant power factor control, direct voltage control, or Volt/var droop control were still being applied to the current distribution networks.

The local Volt/var control methods have been drawn significant attention from many researchers [1]-[15] and widely admitted in most grid codes. For example, Verband Deutscher Elektrotechniker (VDE) in Germany proposed several Volt/var control methods [16] such as the reactive power-voltage curve *Q(V)*, idle power curve as a function *Q(P)* of reactive power (*Q)* with respect to active power injection (*P)*, fixed reactive power, and fixed power factor *(PF)*. Among them, the curve based methods (i.e. *Q(V)* and *Q(P)* curves) are local Volt/var droop control strategies. Their specification of set-points is possibly preset in the course of planning and adjusted via remote control technology or manually. The voltage droop control with its particular advantages is a preferable choice of DNOs and it is officially stipulated, for example, in the UK grid code [17].

Several studies have proposed different Volt/var droop control methods, but, in most of the cases, they were focused on a deterministic framework. The authors in [6] propose a variable droop gain control scheme that mitigates voltage variations at the point of common coupling (PCC). A centralized controller is proposed in [7] to adjust the *V-Q* characteristics of local controllers. In [8], the approach of effectively utilizing the reactive power generation capacity of other inverters closer to the critical bus is proposed to regulate the critical bus voltage while satisfying the PF requirements. The authors in [14] investigate a small wind turbine equipped with the voltage based droop control strategy to obtain a stable microgrid operation. In [15], a droop control method based on modified P&O algorithm is proposed to obtain the maximum power generated by intermittent energy sources such as PV systems or wind turbines.

In work [18], it is found that among local control methods the voltage droop control generally provides better performance in voltage variation, the regulating range of on-load tap changer (OLTC), and minimization of the losses. The voltage droop control method is commonly defined with a fixed gain which is the ratio of the steady-state change in voltage and reactive power. However, in specific cases of a certain network, it is still a big challenge in how to specify optimal gains for local controllers.

In this paper, the approach based on a probabilistic framework is presented to estimate the optimal characteristic curve of Volt/var droop control methods. The optimization objective is active power loss minimization while satisfying operating constraints such as the voltage, loading, and reactive power limits. Monte Carlo (MC) simulation is selected to consider significant uncertainties in inputs such as loads, wind speed, and outage of WGs. A heuristic optimization algorithm is adopted to take account of optimal data points of WGs' reactive power supply. Finally, the approach based on non-linear least squares is used to approximate the optimal characteristic curve which fits best the optimal data points.

To demonstrate the efficiency of the proposed approach, the following droop control methods are investigated in this paper. They are defined in basis on four possible characteristics stipulated in the grid codes [16] and [17], as follows:

- Reactive power versus voltage *Q(V)*
- Power factor (PF) versus voltage *PF(V)*
- Power factor versus active power *PF(P)*
- Reactive power versus active power *Q(P)*

This paper is set out as follows: Section II describes the methodology of the proposed method as well as its crucial parts in detail. Simulation results and discussion are given in Section III, and conclusions are drawn in Section IV.

2. Proposed Methodology

The framework of the proposed methodology is schematically illustrated in Fig. 1. The methodology begins with specifying probabilistic distribution functions (PDFs) of input variables such as power generation of WGs and loads, by depending on their historical measurement data. Next, each trial input scenario sampled from the PDFs defines an operating state. Optimal control variables, reactive power of WGs, are then determined by implementing a heuristic optimization algorithm into load flow calculation. Necessary data making up an output scenario is stored at every MC trial of a total of 12,500 trials (e.g. *Ntr* =12,500) in this paper. Corresponding to each type of droop control method, data points of a different pair of two variables taken from the output scenarios are used. Then these points are approximately fitted by using the approach of non-linear least squares to create the optimal curve from a probabilistic point of view. A pair of two variables of the reactive power (Q) and the voltage (V) is graphically displayed as an example in Fig. 1.

2.1. Distribution Network Model

Load demand variability and WG output are two types of input uncertainties considered in this paper. While load demand is considered as a continuous process, WG output involves either a continuous process, wind speed variability, or a discrete process, failure/operation status of WG. There is the fact that kinds of these continuous uncertainties characterized through a normal probability distribution function (PDF) often supply a very low efficiency. Thus, this paper aims at highlighting a more effective technique, Gaussian mixture model (GMM) approximation, to model such variability.

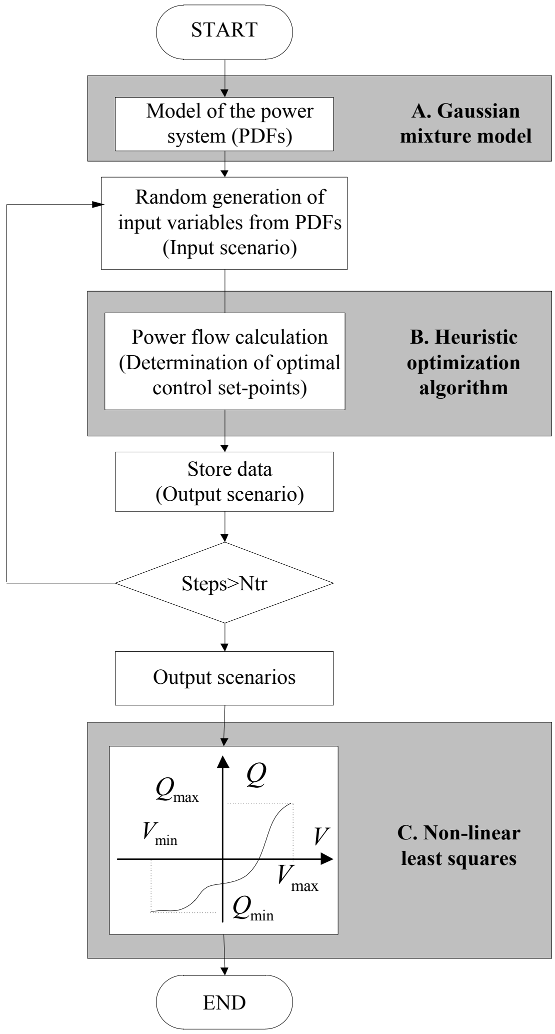

Fig. 1. The framework of the proposed methodology.

Mathematically, the GMM model is represented as a weighted sum of M component Gaussian probabilistic densities [19]-[20]:

$$p(\boldsymbol{x}|\boldsymbol{\lambda}) = \sum_{i=1}^{M} \omega_i g(\boldsymbol{x}|\boldsymbol{\mu}_i, \boldsymbol{\Sigma}_i) \tag{1}$$

where $\boldsymbol{x}$ denotes D-dimensional continuous-valued data vector, $\boldsymbol{\lambda}$ is chosen from the set of parameters $\left\{\boldsymbol{\lambda} : \boldsymbol{\lambda} = \left\{\omega_i, \boldsymbol{\mu}_i, \boldsymbol{\Sigma}_i\right\}_{i=1}^{M}\right\}$, ω_i, *i=1,..., M*, are the mixture weights, and $g(\boldsymbol{x}|\boldsymbol{\mu}_i, \boldsymbol{\Sigma}_i)$, *i=1,..., M*, are the component Gaussian densities. The form of each component density is a D-variate Gaussian function as follows.

$$g(\boldsymbol{x}|\boldsymbol{\mu}_i, \boldsymbol{\Sigma}_i) = \frac{1}{(2\pi)^{\frac{D}{2}} |\boldsymbol{\Sigma}_i|^{\frac{1}{2}}} e^{\left\{-\frac{1}{2}(\boldsymbol{x}-\boldsymbol{\mu}_i)' \boldsymbol{\Sigma}_i^2 (\boldsymbol{x}-\boldsymbol{\mu}_i)\right\}} \tag{2}$$

with $\boldsymbol{\mu}_i$ and $\boldsymbol{\Sigma}_i$ is a mean vector and a covariance matrix, respectively. The mixture weights satisfy the constraint that the sum of all the weights must equal one.

A special routine, written to perform mixture reduction and merging [19], together with the Matlab functions *gmdistribution.fit* (expectation-maximization algorithm - EM) and *chi2gof* (Chi-square goodness-of-fit tests) [21], was used in this paper to identify and validate the parameters of the GMMs.

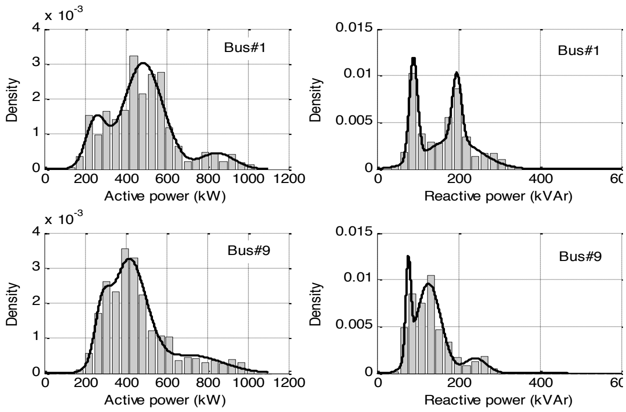

Fig. 2. Probability distributions of nodal active and reactive power demands.

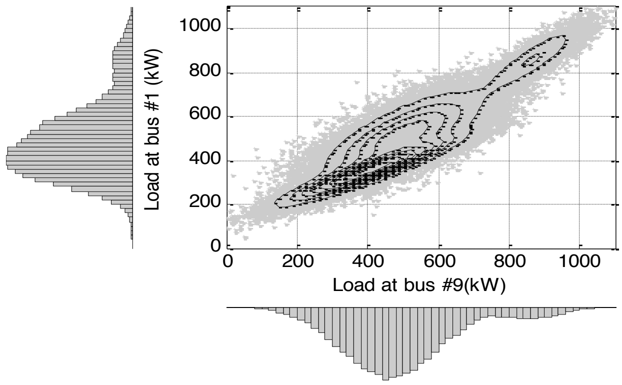

Fig. 3. Bivariate GMM approximation with three mixture components.

2.2. PDF of Load Demand

GMMs are selected to construct PDF of load profile. Firstly the load profile must be required and is calculated as proposed in [19]. Based on available data of load demand for different classes of consumers in each bus, load profile indexes (LPIs) are defined as follows:

$$P_i(t) = \sum_{j=1}^{N_c} \frac{P_{i,max}^j}{\max(P_{PI}^j(\tau))} P_{PI}^j(t) \quad (3)$$

$$Q_i(t) = \sum_{j=1}^{N_c} \frac{P_{i,max}^j}{\max(P_{PI}^j(\tau))} P_{PI}^j(t)\tan(\phi^j) \quad (4)$$

where $P_i(t)$ and $Q_i(t)$ is active power and reactive power load at the *i*th bus, respectively. t, τ is the time instances corresponding to every sampling period (e.g. hour or half-hour, etc), $P_{PI}^j(\tau)$ is the active power value of the LPI of the *j*th class of consumer, $P_{i,\max}^j$ is the annual maximum load. ϕ^j is the angle of average power factor and N_c is the number of consumer classes.

In this paper, historical databases of different classes of consumers in [22] are used to calculate a profile of load demand, with a nominal power of 1 MW of each load bus. For a visual demonstration, the active power and reactive power of only two selected buses are presented in Fig. 2. Correlation about active power of two these buses are effectively handled through EM algorithm, and shown in Fig. 3.

2.3. PDF of WG

PDF of WGs is defined by cooperation between wind speed model and wind generator model as shown in Fig. 4.

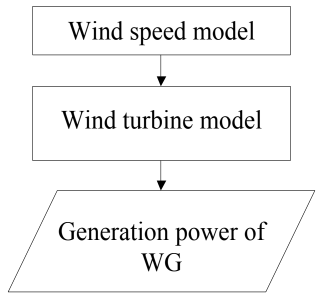

Fig. 4. Model of power generation from WGs.

- *Wind speed:* The GMM approximation from measured wind speed data is illustrated in Fig. 5.

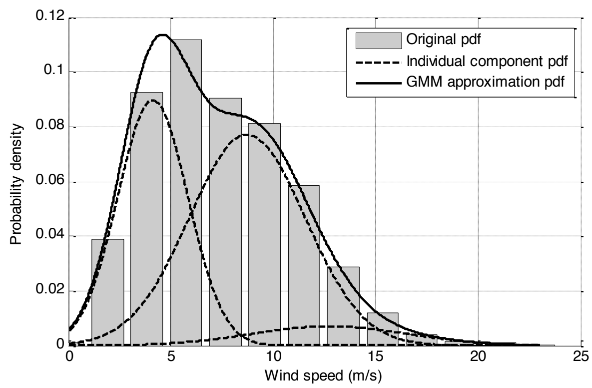

Fig. 5. GMM approximation for wind speed PDF.

- *Wind generator model:* The wind generator model defines its output characteristics and operation status. The value of the power generation is determined by the wind speed and the $P(v)$ characteristic, with cut-in and cut-out wind speed at 3m/s and 25 m/s, respectively.

$$P(v) = \frac{1}{2} C_p \rho A v^3 \quad (5)$$

where C_p is a coefficient of performance, ρ is the air density, A is rotor swept area, and v is wind velocity.

The operation status of every WG is in this paper described by two discrete PDFs of the probability of failure (P_F) and the probability of operation (P_O). While T_F is the statistical time in a failure state, T_O is in an operation state. Their values are given in Table 1.

$$P_F = \frac{T_F}{T_F + T_O}, \quad P_O = \frac{T_O}{T_F + T_O} \tag{6}$$

Table 1. Outage time period per WG of the sub-assemblies [23]

Sub-assemblies	The average annual number of failures	The down-time per failure (hour)	Total annual hours out
Electrical unit	0.551	36	19.84
Control and sensors	0.651	81.6	26.78
Hydraulics	0.27	31.2	8.42
Yaw system	0.25	60	15
Brakes and gearbox	0.33	223.2	34.06
Generator	0.13	139.2	18.10
Structure and drive train	0.22	240	25.92

2.4. Determination of Optimal Control Set-points

Optimal set-points of all available controllable Var sources, reactive power generation of WGs, for minimization of the losses should be determined to meet steady-state Volt/var operational requirements for every input scenario. The mean-variance mapping optimization technique (MVMO) in [24] is used to handle the optimization problem in this paper. The problem is mathematically formulated as follows:

$$OF = P_{loss} = \sum_{k=1}^{N_l} P_k \tag{7}$$

where P_{loss} is a sum of the active power losses of all kth line, P_k, k=1,…, N_l. N_l is the number of distribution network lines. And P_k is calculated as follows:

$$P_k = G_{ij}\left(V_i^2 + V_j^2 - 2V_iV_j\cos\delta_{ij}\right) \tag{8}$$

Subject to

- Voltage at the buses: $V_i^{\min} \le V_i \le V_i^{\max}$ (9)

- Transformer currents: $I_j \le I_j^{\lim}$ (10)

- Line power flows: $S_k \le S_k^{\lim}$ (11)

- Reactive power of WGs: $Q_{WGi}^{\min} \le Q_{WGi} \le Q_{WGi}^{\max}$ (12)

where G_{ij} is the conductance and δ_{ij} is the difference in the voltage angle between the ith bus and jth bus, respectively.

2.5. Approximation of the Optimal Characteristic Curves of WGs

The predefined number of MC simulation trials offers the corresponding number of optimized output scenarios from which two-dimensional target data points are taken for characteristic line approximation. As a result, 12,500 optimal data points ($x_{1..m}, y_{1..m}$) are available for the approximation process. The characteristic curve of the droop control methods in this paper evolving either linear or nonlinear curve is mathematically formulated as follows:

❖ *The linear curve:* A linear curve can be mathematically formulated from two distinct points as shown in (13); therefore, the linear curve can be realized by specifying two of these distinct points, $A(x_A, y_A)$ and $B(x_B, y_B)$.

$$f(x_i, \boldsymbol{\beta}) = y_i = y_A + (y_A - y_B) \times \frac{x_i - x_A}{x_A - x_B} \tag{13}$$

where β is a set of estimated parameters $\{\beta : \beta = \{V_{opti}, \alpha\}\}$ which is used to calculate coordinates of points $A(x_A, y_A)$ and $B(x_B, y_B)$ as shown in Fig. 6 with $d = Q_{\min} / \tan(\alpha)$.

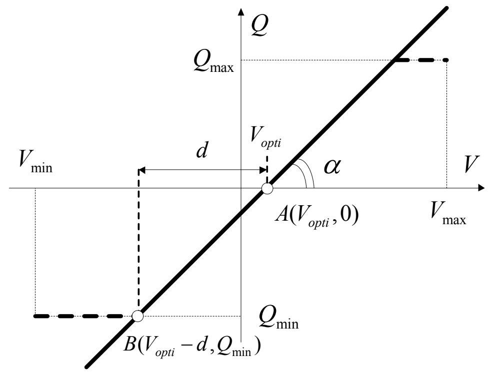

Fig. 6. A linear curve through two distinct points A and B.

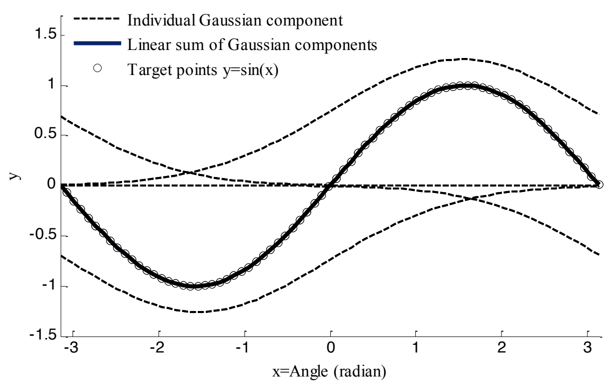

Fig. 7. A curve fitting data points of a function y=sin(x).

❖ *The nonlinear curve:* The nonlinear curve in this paper is defined as a linear sum of the predetermined number of Gaussian functions.

$$f(x_i,\boldsymbol{\beta}) = \sum_{j=1}^{n} \omega_j \frac{1}{\Sigma_j \sqrt{2\pi}} e^{-\frac{1}{2}\left(\frac{x_i-\mu_j}{\Sigma_j}\right)} \qquad (14)$$

$$(i = 1,\dots,m)$$

where $\boldsymbol{\beta}$ is a set of estimated parameters $\left\{\beta : \beta = \{\omega_i, \mu_i, \Sigma_i\}_{i=1}^{n}\right\}$, a member of which defines a Gaussian function, $\omega_i, \mu_i, \Sigma_i$ is weight, mean, and deviation of the ith Gaussian function, respectively and n is the number of Gaussian functions.

- *The approach for nonlinear curve approximation:* The set of estimated parameters $\boldsymbol{\beta}$ in two cases of linear and nonlinear curves presents a non-linear optimization problem. This problem can be handled by the non-linear least-squares approach. Following this approach, for approximating the line $f(x_i,\boldsymbol{\beta})$ which fits optimal data points (x_i, y_i), the quadratic minimization problem must be solved.

$$g(\boldsymbol{\beta}) = \sum_{i=1}^{m} r_i^2(\boldsymbol{\beta}) \qquad (15)$$

where $r_i(\boldsymbol{\beta}) = y_i - f\left(x_i,\boldsymbol{\beta}\right)$

Fig. 7 presents an example of fitting data points derived from a function y=sin(x) to illustrate the efficiency of the proposed approximation approach and of defining a curve through a linear sum of Gaussian functions.

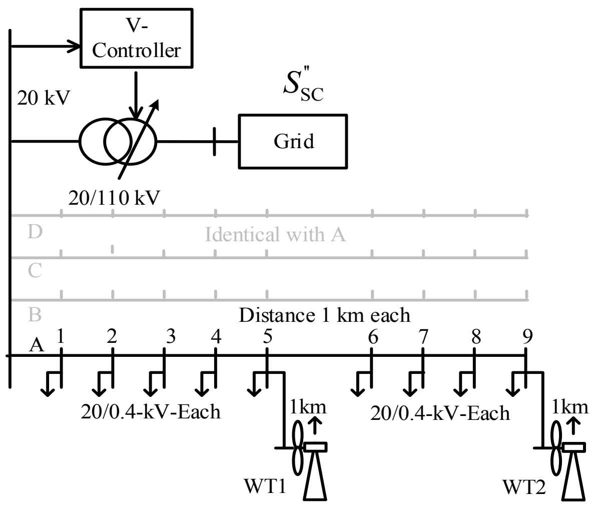

Fig. 8. One-line diagram of the system under study.

3. Simulation Results and Discussion

3.1. Test network

For this study, a generic medium voltage network with a rated voltage of a 20 kV distribution test system and with four identical feeders fed from a 110 kV transmission system is tested. A single-line diagram of the network is shown in Fig. 8. Distances of two adjacent buses are equal to 1km. The maximum load at every load bus is 1MW. WG generation units are connected to bus#5 and #9 with their capacity of 2.0 MW for each. The transformer with an on-load tap-changer is equipped with an automatic voltage regulator (AVR) to keep a given voltage set-point on the low voltage side. For more details, the specification of the network is displayed in Appendix B.

3.2. Impact of Voltage Set-point of the Transformer

The voltage set-point is optimal if it cannot only ensure network operation in operational and security limits but also minimize the losses by setting the network operation close to maximum admissible voltage, the upper boundary of ±10% nominal voltage in distribution networks. To make sure that operating the network in the operational voltage area, the voltage set-point of the transformer must be predefined from worst-case scenarios, over-voltage worst-case (minimum load demand and maximum power generation), and under-voltage worst-case (maximum load demand and no generation). Minimum and maximum load demand were calculated and discussed in previous sections.

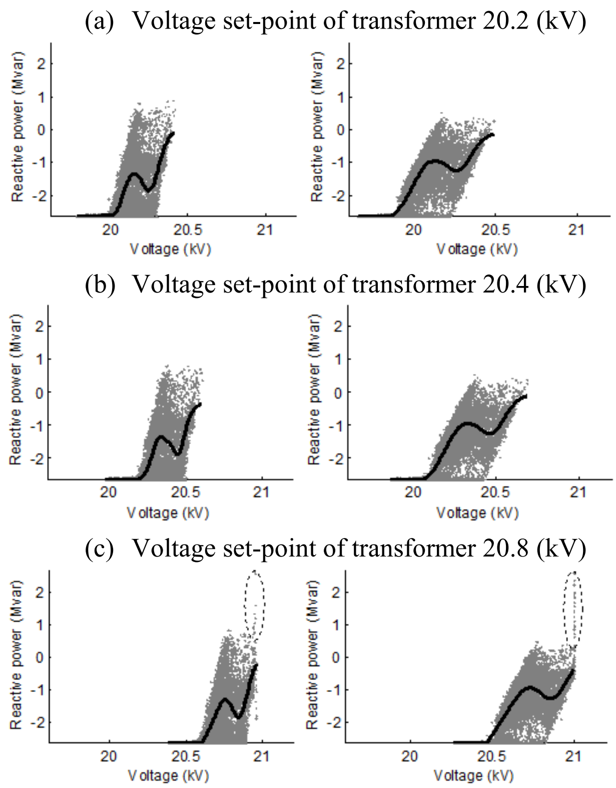

Fig. 9. The characteristic curves of WG1 (left side) and WG2 (right side) approximated corresponding to different voltage set-points of the transformer.

To study the impact of the voltage set-point, the MC simulation is independently performed with three different predefined voltage set-points of the transformer, 20.2 kV, 20.4 kV, and 20.8 kV. The results in response are displayed in Fig. 9 (a), (b), (c) respectively, where scattered points are optimal data points taken from the output scenarios and black dashed line is the approximated characteristic curve.

It can be seen from Fig. 9 is that shape of the optimal characteristic curve is generally unchanged with the variation of voltage set-point of the transformer, and that magnitude of change in the voltage set-point is accompanied by the same magnitude in a shift of the curve.

(a) Reactive power versus voltage Q-V (nonlinear curve)

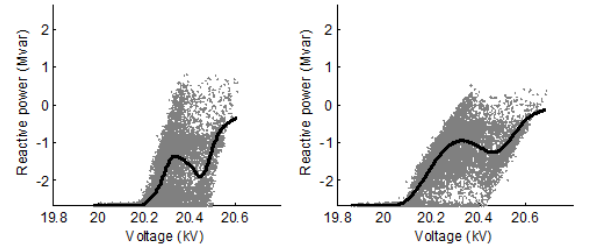

(b) Reactive power versus voltage Q-V (linear curve)

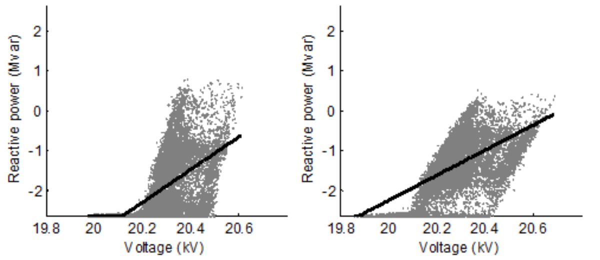

(c) Power factor versus voltage PF-V

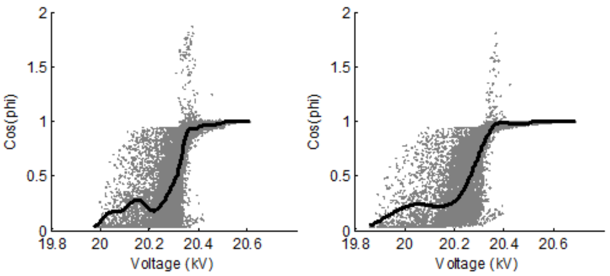

(d) Power factor versus active power PF-P

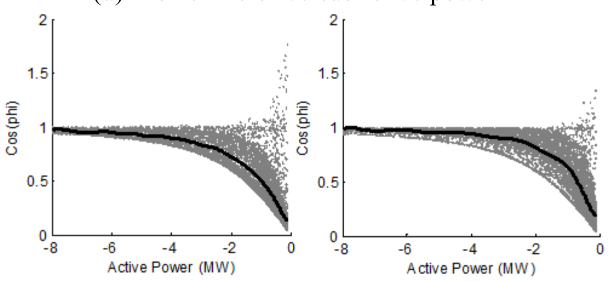

(e) Reactive power versus active power Q-P

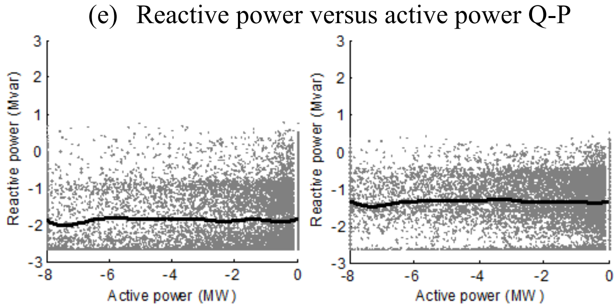

Fig. 10. The characteristic lines of WG1 (left side) and WG2 (right side) approximated corresponding to the droop control methods.

3.3. Approximated Characteristic Curves of the Droop Control Methods

The characteristic curves, black dashed curves, in Fig. 10 are approximated in the case of V_{tap}=20.4 (kV). Note that power factors in Fig. 10 (c) and (d), which are greater than 1, indicate that they are inductive power factors.

Fig. 10 denotes a clear picture of optimal reactive power dispatch in the given distribution network. Generally, the network always requires reactive power injection from WGs for its optimal operation. This makes up a conflict with provisions, settled in some grid codes, about the definition of the characteristic curve, where WGs must be set for either reactive power generation or absorption in operational voltage area.

3.4. Comparative Efficiency between the Droop Control Methods

❖ *The losses:* Minimization of the losses is an important task in any aspect of power system planning, and it is also considered in this paper as the main optimization objective. The losses resulting from the droop control methods and two cases of 0.95 capacitive and unity fixed PF are compared in Table 2.

Table 2. The annual losses (MWh)

Q-V (nonlinear)	Q-V (linear)	PF-V	PF-P	Q-P	PF=1	PF=0.95 (cap.)
1,155	1,159	1,166	1,184	1,170	1,252	1,226

It can be seen that the losses are reduced the most by the implementation of the Q-V voltage droop control method into WGs. Approximation of characteristic curves depending on linear curves causes increased approximation error from ideally optimized curves resulting in slightly higher losses. Nonetheless, it may be expected that if the larger reactive capacity of WGs may lead to the larger error, these increased losses are much higher over the year.

The PF-V droop control method has recently obtained the expectation of engineers in improving control efficiency, but the results demonstrated adverse impact. This is because reactive power generation of WGs from a full range [0-1] of reference PFs to capture the optimal nonlinear curve is not fulfilled in many scenarios due to reactive power capacity limit of WGs, only 33.33% nominal power of WGs.

Droop control methods depending on voltage always achieve better optimization efficiency than that depending on active power generation. This is because voltage can reflect the stochastic variation of all input variables such as load demand and power generation.

It can also be seen that the losses in the droop control methods are significantly lower than the losses incurred when WGs are set by a typical scenario of 0.95 capacitive and unity power factor.

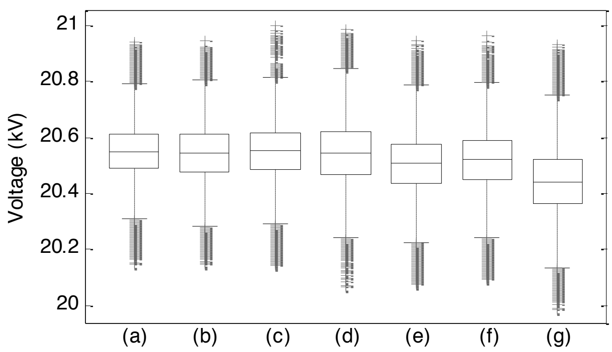

Fig. 11. Box plot of the voltage at bus#9: (a) Q-V(nonlinear curve), (b) Q-V (linear curve), (c) PF-V, (d) PF-P, (e) Q-P, (f) PF=1, (g) PF=0.95 (Cap.).

❖ *Voltage profile:* Box plot is selected to present statistical results of voltage in this paper, because it provides a clearer picture of the differences between groups of numerical data, as shown in Fig. 11.

It can be seen that the voltage droop control with Q-V linear curves offers the best performance in voltage quality due to its narrowest operational voltage area. In contrast, the method PF-P in (d) is the worst among the droop control methods with an increased risk of overvoltage violation.

The methods of voltage droop control lead to better reduction in voltage variation than these of active power droop control. This is because the active power droop control methods always ignore the impact of load demand, the significant uncertainty.

4. Conclusion

This paper introduces the effective framework based MC simulation considering all significant uncertainties of the distribution network to approximate the optimal characteristic curves of droop control methods implemented into WGs. Among the droop control methods, the voltage droop control with Q-V nonlinear curves presents the best performance via its effective ability not only in minimizing the losses but also in reducing voltage variation. With slightly lower performance, the Q-V linear curve is still recommended to apply to the given network due to its computational benefit and its easier implementation into WGs.

In comparison to the traditional fixed power factor method, the voltage droop control methods present much better performance. Therefore it should obtain more attention from DNOs.

Acknowledgements

This paper was fully funded by Tra Vinh University.

References

[1] A. Keane, L.F. Ochoa, E. Vittal, C.J. Dent, and G.P. Harrison, “Enhanced utilization of voltage control resources with distributed generation”, IEEE Trans. Power Syst., vol. 26, no. 1, pp. 252–260, Feb. 2011.

[2] T. Sansawatt, L.F. Ochoa, and G.P. Harrison, “Smart decentralized control of DG for voltage and thermal constraint management”, IEEE Trans. Power Syst., vol. 27, no. 3, pp. 1637–1645, Aug. 2012.

[3] R. Aghatehrani, and R. Kavasseri, “Reactive power management of a DFIG wind system in microgrids based on voltage sensitivity analysis”, IEEE Trans. Sustainable Energy, vol. 2, no. 4, pp. 451–458, Oct. 2011.

[4] S.B. Kim and S.H. Song, “A hybrid reactive power control method of distributed generation to mitigate voltage rise”, Energies, vol. 13, no. 2078, Apr. 2020.

[5] D.L. Schultis, “Comparison of local volt/var control strategies for PV hosting capacity enhancement of low voltage feeders”, Energies, vol. 12, no. 1560, Apr. 2019.

[6] Y. Li, Z. Xu, J. Zhang, and K. Meng, “Variable droop voltage control for wind farm”, IEEE Trans. Sustainable Energy, vol. 9, no. 1, pp. 491–493, Jan. 2018.

[7] H.S. Bidgoli and T.V. Cutsem, “Combined local and centralized voltage control in active distribution networks”, IEEE Trans. Power System, vol. 33, no. 2, pp. 1374–1384, March 2018.

[8] A. Safayet, P. Fajri, and I. Husain, “Reactive power management for overvoltage prevention at high PV penetration in a low-voltage distribution system”, IEEE Trans. Industry Applications, vol. 53, no. 6, pp. 5786–5794, Dec. 2017.

[9] Li, Z. Xu, J. Zhang, and K. Meng, “Variable droop voltage control for wind farm”, IEEE Trans. Sustainable Energy, vol. 9, no. 1, pp. 491–493, Jan. 2018.

[10] M. Zainuddin, F.E.P. Surusa, Syafaruddin, and S. Manjang, “Constant power factor mode of grid-connected photovoltaic inverter for harmonics distortion assessment,” International Journal of Renewable Energy Research (IJRER), vol. 10, no. 3, Sept. 2020.

[11] R. Campaner, M. Chiandone, G. Sulligoi, and F. Milano, “Application of new voltage control rules in distribution networks,” In Proc. of 2013 International Conference on Renewable Engergy Research and Applications (ICRERA).

[12] K.A. Khan, and M. Khalid, “A reactive power compensation strategy in radial distribution network with PV penetration,” In Proc. of 2019 International Conference on Renewable Engergy Research and Applications (ICRERA).

[13] E. Avdiaj, J.A. Suul, S. D’Arco, and L. Piegari, “A current controlled virtual sysnchronous machine adapted for operation under unbalanced conditions,” In Proc. of 2020 International Conference on Renewable Engergy Research and Applications (ICRERA).

[14] J.V. de Vyver, T. Feremans, T.L. Vandoorn, F.D.M. De Kooning, and L. Vandevelde, "Voltage based droop control in an islanded microgrid with wind turbines and

battery storage," In Proc. of 2015 International Conference on Renewable Engergy Research and Applications (ICRERA).

[15] E. Irmak, N. Guler, E. Kabalci, and A. Calpbinici, "A modified droop control method for PV systems in island mode DC microgrid," In Proc. of 2019 International Conference on Renewable Engergy Research and Applications (ICRERA).

[16] Technical Connection Rules for Medium-Voltage (VDE-AR-N 4110), Feb. 2017. Available online: https://www.vde.com/en/fnn/topics/technical-connection-rules/tcr-for-medium-voltage (accessed on 04 October 2020.

[17] National Grid, “The grid code,” Issue 4, Revision 2, March 22nd, 2010.

[18] V.H. Pham, J.L. Rueda and I. Erlich, “Probabilistic evaluation of voltage and reactive power control methods of wind generators in distribution networks”, IET Renewable Power Generation, vol. 9, no. 3, pp. 195–206, 2015.

[19] R. Singh, B.C. Pal, and R.A. Jabr, “Statistical representation of distribution system loads using Gaussian mixture model”, IEEE Trans. Power Syst., vol. 25, no. 1, pp. 29–37, Feb. 2010.

[20] G. Valverde, A.T. Saric, and V. Terzija, “Probabilistic load flow with non-Gaussian correlated random variables using Gaussian mixture models”, IET Gener. Transm. Distrib., vol.6, Iss. 7, pp. 701-709, Jan. 2012.

[21] “Matlab Statistical Toolbox, User’s Guide.” Available: http://www.mathworks.com.

[22] The United Kingdom Generic Distribution Network. Available: http://monaco.eee.strath.ac.uk/ukgds/.

[23] Institut für Solare Energieversorgungstechnik, “Windenergy Report Germany 2008”.

[24] I. Erlich, G. K. Venayagamoorthy, and W. Nakawiro, " A mean-variance optimization algorithm", Proc. 2010 IEEE World Congress on Computational Intelligence, Barcelona, Spain.